JOURNAL OF SOLID STATE CHEMISTRY 106, 349–356 (1993)

Thermochemical Study of Ln_2O_3, T'-Ln_2CuO_4, and $Ln_2Cu_2O_5$ (Ln = Rare Earth)

E. TAKAYAMA-MUROMACHI*

National Institute for Research in Inorganic Materials (NIRIM), 1-1 Namiki, Tsukuba, Ibaraki, 305 Japan

AND A. NAVROTSKY

Department of Geological and Geophysical Sciences and Princeton Materials Institute, Princeton University, Princeton, New Jersey 08544

Received September 9, 1992; in revised form January 13, 1993; accepted January 19, 1993

High temperature solution calorimetry using a $2PbO \cdot B_2O_3$ solvent at 977 K was applied to the high T_c-related compounds, Ln_2O_3 (Ln= Nd–Lu), T'-Ln_2CuO_4 (Ln = Nd–Gd), and $Ln_2Cu_2O_5$ (Ln= Dy–Lu). The heat of solution, ΔH_s, of Ln_2O_3 becomes less exothermic with decreasing size of Ln^{3+} from ~−130 kJ/mole in La_2O_3 to ~−30 kJ/mole in Lu_2O_3. The heats of solution of rare earth oxides containing unevenly filled "4f" orbitals are slightly more endothermic than those predicted by a straight line relating ΔH_s to reciprocal ionic radius, $1/r$, for La, Gd, Y, and Lu, presumably reflecting the crystal field stabilization energy of Ln^{3+} (CFSE) in the solid. The heat of solution of the T' phase when plotted against $1/r$ shows a maximum value at Ln= Sm. This may be explained by the CFSE and/or by a nonlinear change in lattice energy of the T' phase as a function of $1/r$. The stability relations between T' and $Ln_2Cu_2O_5$ structures are discussed using the thermochemical data obtained. The data generally confirm patterns of stability seen in synthesis experiments.

Introduction

The Ln_2CuO_4 (Ln = rare earth) compounds crystallize in the T'-type structure for Ln = Pr, Nd, Sm, Eu, Gd at ambient pressure. The T' structure is closely related to the T-type (K_2NiF_4-type), in which La_2CuO_4 crystallizes. The metal positions are essentially the same in these structures but the oxygen positions are different (*1*). Copper assumes square planar coordination in the T' structure but octahedral coordination in the T structure. The lanthanide, on the other hand, occupies a cubic 8-coordinated site in the former and a 9-coordinated site in the latter. The T' compound has attracted a great deal of attention since it becomes an n-type superconductor with T_c ~30 K after being doped with Ce (*2*).

Rare earth cations smaller than Gd^{3+} can not form the T'-type structure at ambient pressure and there appears, instead, a $Ln_2Cu_2O_5$ phase (225 phase) in the pseudobinary system of CuO–Ln_2O_3 (Ln = Y, Tb–Lu). In the 225 structure, the rare earth atom and the Cu atom occupy highly distorted sites, namely distorted octahedral and distorted square planar, respectively (*3*). Okada *et al.* (*4*) and subsequently Bordet *et al.* (*5*) have shown that the T' structure becomes stable under high pressure even for rare earth cations having smaller sizes (Ln = Y, Tb, Dy, Ho, Er, Tm).

Very recently, Mocala *et al.* applied high-temperature solution calorimetry to the $(La_{1-x}Nd_x)_2CuO_4$ system which shows the T'-to-T transition with decreasing Nd con-

* To whom correspondence should be addressed.

0022-4596/93 $5.00

tent, x (*6*). They found that enthalpy change of the T'-to-T transition in La_2CuO_4 is very small (near 3 kJ/mole).

In the present study, the heats of solution in molten $2PbO \cdot B_2O_3$ at 977 K of the series of compounds, Ln_2O_3 (Ln = Nd–Lu), T'-Ln_2CuO_4 (Ln = Nd–Gd), and $Ln_2Cu_2O_5$ (Ln = Dy–Lu) have been measured. The thermochemical data are discussed in terms of the ionic radius of the Ln ion, which appears to be the most important crystal chemical factor governing the stability relations among the phases in the CuO–Ln_2O_3 systems.

Experimental

Sample Preparation

All samples were prepared at NIRIM by usual solid state reactions. Rare earth oxides Ln_2O_3 (Ln = Nd–Lu, 99.9%) and CuO (99.9%) were dried at 1273 and 1073 K, respectively and then used as starting reagents. The T' compounds with Ln= Nd, Sm, Eu, Gd were prepared at 1373 K for 4 days with an intermediate grinding. To remove oxygen defects, the products, after being thoroughly ground, were placed in an O_2-flow furnace and slowly cooled from 1173 K to room temperature. The 225 compounds with Ln = Dy, Ho, Er, Tm, Yb, Lu were prepared at 1273 K for 4 days with an intermediate grinding and then cooled in a furnace in air. All samples thus obtained were examined by powder X-ray diffractometry using Cu$K\alpha$ radiation. No extra peaks were found in their X-ray patterns. Pr_2CuO_4 and $Tb_2Cu_2O_5$ were omitted from the present study since oxidation states in the lead borate solvent are not known for the Pr and the Tb ions and oxidation states even in the binary oxides are complicated.

Solution Calorimetry

Solution calorimetric measurements were performed at Princeton. The high temperature twin Calvet-type solution calorimeter and the technique used have been described elsewhere (*7*). A sample of 15–30 mg was dissolved into molten $2PbO \cdot B_2O_3$ solvent after being equilibrated for 6–15 hr in the calorimeter maintained at 977 K. Solution calorimetry using the lead borate solvent has been widely applied to oxide systems (*7*). It was, however, previously found that rare earth oxides in normal powder form do not always dissolve completely in the lead borate solvent but often tend to form a rare earth borate precipitate (*6, 8*). This precipitate appears to be metastable, and its formation and redissolution seem to depend on locally saturating the solvent during the initial reaction. To avoid this problem, a special technique in sample preparation has been reported to be effective. The rare earth oxide was dissolved in nitric acid then was carefully heated. The very porous (though well crystallized) sample thus obtained was successfully dissolved in the lead borate solvent (*6, 8*).

The rare earth oxide is, however, not an easy sample for the lead borate solvent even using the above-mentioned technique. In the present study, we adopted a different technique because a cross check of data with a different method is desirable. We prepared a mechanical mixture of the rare earth oxide with CuO in 1 : 1 or 1 : 2 mole ratio (Ln_2O_3 : CuO) by grinding in an agate mortar. Because of very fast dissolution kinetics of CuO in the solvent, we expected that the rare earth oxide would be dispersed in the solvent and precipitate formation would be suppressed. Indeed, it was found that the mixture did dissolve readily in the solvent with less vigorous stirring. The heat of solution of the rare earth oxide was calculated by subtracting the heat effect of CuO from that of the mixture.

To check if chemical reaction occurred between CuO and Ln_2O_3 during the equilibration period in the calorimeter, every mixture was maintained at 977 K for 24 hr and then was identified by powder X-ray diffraction. In the cases Ln = Nd and Sm, trace amounts of Nd_2CuO_4 and Sm_2CuO_4 (~5%) were found in the X-ray patterns. The heat

of solution of Nd_2O_3 or Sm_2O_3 were corrected for the impurity phases but the correction was only ~0.5 kJ/mole. The heat of solution of Nd_2O_3 in the present study is in good agreement with the previous value obtained for the porous sample (see below).

The T' or 225 compounds could be dissolved in the solvent using the standard technique. However, we applied the mixing method to them as well, since less vigorous stirring was needed for the CuO-mixed samples.

Lattice Energy Calculation of T' Phases

Madelung energies of the T' compounds were calculated by means of the standard Ewald method. The T' structure belongs to the tetragonal space group $I4/mmm$ and the z-position of the Ln atom is the only variable internal parameter in the atomic coordination (*1*). The z-value has been reported for three T' samples, Ln= Nd (*9*), Gd (*9*), Tm (*5*). They increase with the ionic radius of the Ln ion from 0.34579 (Tm) to 0.35117 (Nd). We assumed a linear relationship between the z-value and the ionic radius and estimated the z-values of other T' compounds. For Tm_2CuO_4, complicated superlattice reflections were observed in electron diffraction patterns (*5*). In addition, it is suggested that oxygen site in the CuO_2 layer (O(1) site) is slightly displaced along the a-axis from the ideal 4c position in Gd_2CuO_4 (*9*) and Tm_2CuO_4 (*5*). In the Madelung energy calculation, we neglected these complications. This approximate treatment seems accurate enough to discuss relative change of Madelung energy as a function of ionic radius of Ln ion (see below). Lattice parameters used in the present calculation were taken from literature cited in Ref. (*10*).

The short range interaction between Cu and O in a T' compound was calculated based on the Buckingham potential,

$$V(r') = A \exp(-r'/\rho) - C/r'^6$$

using the Cu–O bond length r' calculated from the a-dimension and the parameters A = 294.15 eV, ρ = 0.40023 Å, C = 0.0 eV Å^{-6} given by Islam *et al.* (*11*).

TABLE I

HEAT OF SOLUTION IN 2PbO · B_2O_3 AT 977 K, ΔH_s AND HEAT OF FORMATION FROM OXIDES AT 977 K, ΔH_f(ox) OF CuO, Ln_2O_3, T'-Ln_2CuO_4 AND $Ln_2Cu_2O_5$

Compounds	ΔH_s (kJ/mole)[a,b]	ΔH_f(ox) (kJ/mole)[a]
CuO	33.3 ± 0.4[c]	
	33.5 ± 0.4(6)	
Y_2O_3	−61.7 ± 1.1[d]	
La_2O_3	−126.0 ± 4.4[c]	
Nd_2O_3	−89.1 ± 5.7[e]	
	−85.1 ± 3.7(4)	
Sm_2O_3	−79.4 ± 4.1(6)	
Eu_2O_3	−68.4 ± 1.3(6)	
Gd_2O_3	−72.6 ± 3.4(4)	
Dy_2O_3	−50.9 ± 1.2(5)	
Ho_2O_3	−50.2 ± 5.6(6)	
Er_2O_3	−47.6 ± 1.7(5)	
Tm_2O_3	−47.1 ± 2.8(5)	
Yb_2O_3	−39.5 ± 1.9(5)	
Lu_2O_3	−34.4 ± 1.2(5)	
Nd_2CuO_4	−41.5 ± 1.9[e]	−14.3 ± 6.0[e]
	−38.2 ± 1.6(6)	−13.4 ± 4.1
Sm_2CuO_4	−26.2 ± 3.3(6)	−19.7 ± 5.3
Eu_2CuO_4	−33.0 ± 3.2(5)	−1.9 ± 3.5
Gd_2CuO_4	−38.8 ± 4.3(5)	−0.3 ± 5.5
$Y_2Cu_2O_5$	−0.2 ± 1.7[d]	5.1 ± 2.2[d]
$Dy_2Cu_2O_5$	7.1 ± 2.7(6)	9.0 ± 3.0
$Ho_2Cu_2O_5$	9.0 ± 1.3(6)	7.8 ± 5.8
$Er_2Cu_2O_5$	9.7 ± 2.9(5)	9.7 ± 3.4
$Tm_2Cu_2O_5$	20.1 ± 3.6(5)	−0.2 ± 4.6
$Yb_2Cu_2O_5$	21.1 ± 4.6(7)	6.4 ± 5.0
$Lu_2Cu_2O_5$	29.8 ± 5.7(5)	2.8 ± 5.9

[a] Error is indicated by two standard deviation of mean.
[b] Number in ( ) is number of experiment performed.
[c] Taken from Ref. (*8*).
[d] From Ref. (*14*).
[e] From Ref. (*6*).

Results and Discussion

Heat of Solution of Ln_2O_3

Heats of solution of Ln_2O_3 are shown in Table I and Fig. 1, where the values for La_2O_3 and Y_2O_3 were taken from the reports

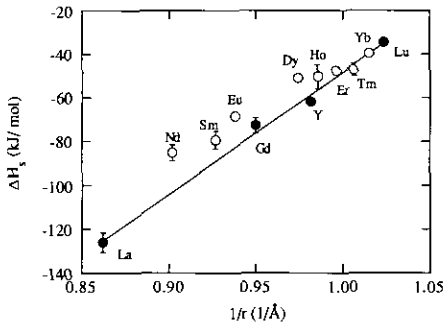

FIG. 1. Heat of solution of Ln_2O_3 as a function of reciprocal of ionic radius of Ln^{3+} ion, $1/r$. The data for La_2O_3 and Y_2O_3 are taken from Refs. (*8*) and (*14*), respectively.

by Bularzik *et al.* (*8*) and by Zhou and Navrotsky (*14*), respectively. At the experimental temperature, 977 K, both La_2O_3 and Nd_2O_3 crystallize in the *A*-type structure and Sm_2O_3 in the *B*-type structure while oxides with Ln = Y, Gd–Lu crystallize in the *C*-type structure (*12*). The heats of solution shown in the table correspond to these structure types (the heat of transition between two structures is generally very small, e.g., ~3 kJ/mole for *B*-to-*C* transition in Sm_2O_3 (*13*)). As described above, the heat of solution of Nd_2O_3 in the present study is in good agreement with the previous value given by Mocala *et al.* (*6*).

To see the influence of the size of the Ln^{3+} on the heat of solution, ΔH_s (Ln_2O_3) is plotted in Fig. 1 as a function of reciprocal of Shannon's ionic radius of Ln^{3+} in 8-coordination, $1/r$ (*15*). The ΔH_s of four oxides, La_2O_3, Gd_2O_3, Y_2O_3, and Lu_2O_3 are located on a straight line while there are significant deviations in the positive direction from the straight line in other rare earth oxides except for Ln = Er, Tm, Yb. Very similar deviations are observed when ΔH_s is plotted against the ionic radius itself or against the atomic number of the rare earth. The rare earth ions in the first four oxides have spherically symmetric shells ($La^{3+}: 4f^0$, $Gd^{3+}: 4f^7$, $Y^{3+}: 4p^6$, $Lu^{3+}: 4f^{14}$) with no crystal field stabilization energy (CFSE). This suggests that the positive deviation described above can be explained by CFSE due to $4f$ electrons of Ln^{3+}.

The coordination polyhedra of the Ln ion in the *A*-, *B*-, or *C*-type Ln_2O_3 are highly distorted from the ideal octahedron or cube (*16*). Nevertheless, it is helpful for qualitative argument to see the *f*-level splitting in a ligand field with simple cubic symmetry. The CFSE for the cube may be expressed by (*17*),

$$\mathrm{CFSE}_{\mathrm{calc}} = (\tfrac{3}{7}n_1 - \tfrac{1}{7}n_2 - \tfrac{6}{7}n_3)14Dq,$$

where n_1, n_2 and n_3 are the numbers of *f* electrons in the t_{1u}, t_{2u}, and a_{2u} orbitals in the cubic eight coordination, respectively and $14Dq$ indicates crystal field strength by analogy with the symbol of *d* electrons, $10Dq$. In Fig. 2, CFSE calculated by the above equation are compared with the deviation of ΔH_s per mole Ln^{3+} from the straight line. This figure suggests some correlation between CFSE and the deviation. In $Nd(BrO_3)_3 \cdot 9H_2O$, the CFSE is estimated to be ~6 kJ/mole (*18*) which has the same order of magnitude as the deviation of ΔH_s for Nd_2O_3, ~9 kJ/mole · Nd^{3+}. From these facts we conclude that the nonlinear relation between $\Delta H_s(Ln_2O_3)$ and $1/r$ is related to the ligand field stabilization of Ln^{3+} in crystalline Ln_2O_3.

More quantitative discussion of CFSE is rather difficult because the deviation in ΔH_s from the straight line does not reflect di-

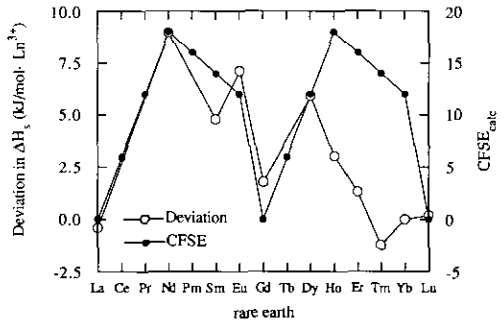

FIG. 2. Deviation of $\Delta H_s(Ln_2O_3)$ from the straight line and crystal field stabilization energies for Ln^{3+} ions in terms of Dq (see text).

rectly CFSE in the solid but reflects the difference in CFSE between the crystalline and molten environment. Unfortunately, no experimental data are available to estimate quantitatively the ligand field strength for the rare earth ion in the lead borate solvent. However, the deviation from the straight line in ΔH_s of the Ln_2O_3 is always positive or close to zero which indicates that CFSE in the melt is smaller in magnitude than that in the solid. The ligand field strength is expected to decrease in the melt because of greater thermal motion of ions, random arrangement of ions and less dense environment. In addition, the oxygen ion is supposed to be strongly bound to the boron ion rather than to the rare earth ion in the lead borate melt which seems to result in the weaker ligand field strength for the rare earth ion.

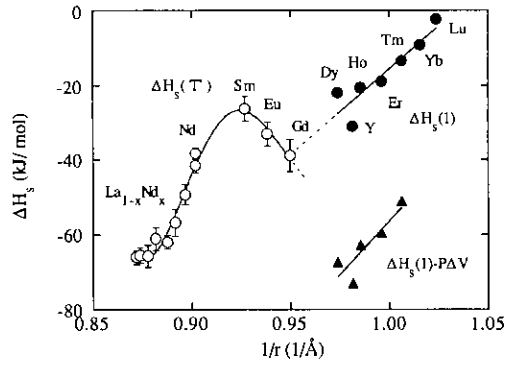

FIG. 3. Heats of solution of the T' phase, $\Delta H_s(T')$ and the mixture of Ln_2O_3 and $Ln_2Cu_2O_5$, $\Delta H_s(1)$ as functions of reciprocal of the ionic radius of Ln^{3+}. The heat of solution of the mixed system is defined by $\Delta H_s(1) = \frac{1}{2}\Delta H_s(Ln_2O_3) + \frac{1}{2}\Delta H_s(Ln_2Cu_2O_5)$. The data for the $(La_{1-x}Nd_x)_2CuO_4$ system were taken from Ref. (*6*). The term $\Delta H_s(1)$-$P\Delta V$ is calculated for P = 8 GPa and volume change ΔV in the reaction,

$$T'\text{-}Ln_2CuO_4 \rightarrow \tfrac{1}{2}Ln_2O_3 + \tfrac{1}{2}Ln_2Cu_2O_5.$$

Energetics of T'-Ln_2CuO_4

Heats of solution and heats of formation from oxides, ΔH_f(ox) of the T' compounds are listed in Table I. The ΔH_s and ΔH_f(ox) for Nd_2CuO_4 in the present study are in good agreement with the previous values by Mocala *et al.* (*6*). Recently, Warner *et al.* examined Nd_2CuO_4 by solid state galvanometry and reported the standard free energy change, $\Delta G°$(400–500 K) = −27300 − 61T J/mole (*19*), for the reaction,

$$Cu + \tfrac{1}{2}O_2 + Nd_2O_3 = Nd_2CuO_4.$$

Their results are, however, extremely doubtful. Combining their results with the thermochemical data for CuO, ΔH_f (500 K) = −154.8 kJ/mole and ΔS_f (500 K) = −90 J/mole · K (*20*), ΔH_f (500 K) and ΔS_f(ox) (500 K) for Nd_2CuO_4 are calculated to be 127.5 kJ/mole and 151 J/mole · K, respectively. This ΔH_f(ox) is completely different from our result. They imply that a surprisingly large positive enthalpy of formation from the oxides is counterbalanced by an equally large entropy change, and that the compound is unstable to decomposition to CuO + Nd_2O_3 below 844 K. This is unreasonable and unlikely. We suggest experimental problems in their study, particularly oxidation of the reference copper electrode.

In Fig. 3, the heats of solution of T' compounds are shown as a function of $1/r$. The previous data on $(La_{1-x}Nd_x)_2CuO_4$ (*6*) are included in the figure using a weighted average of ionic radii of Nd^{3+} and La^{3+}. The heat of solution of the T' compounds increases (becomes more endothermic) with $1/r$ until Ln = Sm and then decreases for larger $1/r$ (for smaller Ln ions).

The CFSE of the Ln ion may be a possible reason for the downturn but this would require a CFSE more than 10 kJ/mole · Ln^{3+} to explain $\Delta H_s(Sm_2CuO_4)$, for instance. This may be too large compared with the results shown in Fig. 2. There is another explanation for the downturn. In Fig. 4, the Madelung energy (E_M) is plotted against $1/r$ for the T' compounds including the phases stable at high pressure. The Madelung energy can be well expressed by two straight lines intersecting at Ln = Sm. The lattice energy consists of not only the long range electrostatic term (Madelung term) but the short range interaction in which the repulsive interac-

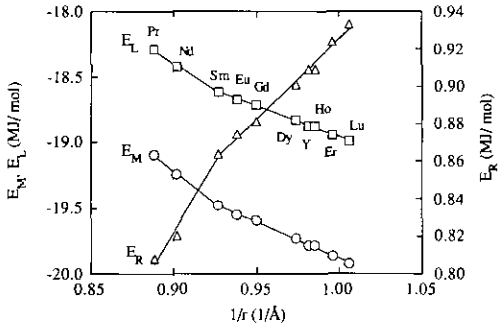

FIG. 4. Variation of the Madelung energy (E_M), the Cu–O short range interaction (E_R) and their summation ($E_L = E_M + E_R$) of the T' phase against the reciprocal of the ionic radius of Ln^{3+}.

tion is a dominant term. As shown in Fig. 5, the Cu–O bond length in the T' structure is almost the same as the sum of ionic radii of Cu^{2+} and O^{2-} when the Ln ion is relatively large (Ln = Pr or Nd), while for smaller Ln ions, the Cu–O distance becomes noticeably shorter than the "ideal" bond length. This suggests that the short range interaction of the Cu–O bond makes a major contribution to the change of lattice energy as a function of $1/r$. The Cu–O short range interaction (E_R) and the sum of the Madelung energy and the Cu–O short range interaction (E_L) are plotted in Fig. 4. Similar to the Madelung energy, each term can be expressed by two intersecting straight lines. The abrupt change of slope in E_L near Ln = Sm is well correlated with the maximum in ΔH_s at Ln = Sm in Fig. 3. It is not strictly correct to separate lattice energy from crystal field effects, since structural data to be used for calculation of lattice energy are already influenced by any crystal field effect. There are, however, no anomalies in E_M, E_R, or E_L at Ln = Y, Gd in Fig. 4. This suggests that the correlation between lattice energy and CFSE is weak enough to discuss them separately in the present case.

Bordet *et al.* (*5*) plotted ratio of cell dimensions (c/a ratio) of the T' compounds as a function of the ionic radius of Ln^{3+}. The ratio increases with the radius in the entire range but the slope of this relation changes drastically at Ln = Sm. This phenomenon may be correlated with the downturn in $\Delta H_s(T')$.

We can not conclude definitely which is the main reason for the downturn, CFSE of Ln^{3+} ion or the nonlinear change of lattice energy. Further work, in particular, calorimetric measurement of the high-pressure T' phases would be helpful to answer the question.

To see the stability relation between the T' phase and the mixed system of $Ln_2Cu_2O_5$ and Ln_2O_3, heat of solution of the mixture $\Delta H_s(1) = \frac{1}{2}\Delta H_s(Ln_2O_3) + \frac{1}{2}\Delta H_s(Ln_2Cu_2O_5)$ is plotted in Fig. 3. If $\Delta H_s(1)$ is assumed to change linearly against $1/r$, the extrapolation of the straight line for the $\Delta H_s(1)$ intersects the $\Delta H_s(T')$ curve near Ln = Gd. This result is compatible with results of synthesis experiments at ambient pressure which show that a T' phase is not stable for the Ln ion smaller than Gd^{3+} but would decompose to 225 phase and Ln_2O_3 according to the reaction,

$$T'\text{-}Ln_2CuO_4 \rightarrow \tfrac{1}{2}Ln_2O_3 + \tfrac{1}{2}Ln_2Cu_2O_5.$$

At high pressures, the T' compound is stabilized against the 225–Ln_2O_3 mixture since the volume change for the above reaction (ΔV) is positive. As a simple treatment, we calculate ΔV using the cell dimensions at ambient pressure (*21*) and the term,

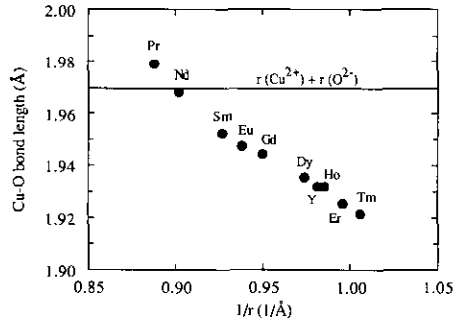

FIG. 5. Cu–O bond length in the T' phase calculated from the a-dimension (*10*) as a function of the reciprocal of the ionic radius of Ln^{3+}. The horizontal line indicates the sum of Shannon's ionic radius of Cu^{2+} in square planar coordination and that of O^{2-} in 6-coordination (*15*).

$\Delta H_s(1) - P\,\Delta V$ for $P = 8$ GPa is plotted in Fig. 3. The ΔH_s curve shifts downward by ca. 40 kJ/mole for 8 GPa and a T' phase is stabilized against the mixture approximately by this amount. This very rough estimation appears to be compatible with high-pressure synthesis experiments by Okada *et al.* (*4*) and Bordet *et al.* (*5*). We need thermochemical data of high-pressure T' phases for more quantitative arguments.

The heat of formation of the T' phase from the oxides is not a smooth function of ionic radius of the Ln ion. Instead of plotting $\Delta H_f(\text{ox})(T')$ against $1/r$, we compared heat of solution of the T' phase and that of the mixture of Ln_2O_3–CuO ($\Delta H_s(2)$) (see Fig. 6). The two curves intersect at Ln = Gd, suggesting that the T' structure becomes unstable not only against the 225–Ln_2O_3 mixture but also against the Ln_2O_3–CuO mixture for Ln ion smaller than Gd^{3+}. The T' phases with the smaller Ln ions would, however, become stable at high pressures since the volume change is positive for the reaction,

$$Ln_2CuO_4 \rightarrow Ln_2O_3 + CuO.$$

Energetics of $Ln_2Cu_2O_5$

The heats of solution and heats of formation from oxides for the 225 phases are listed in Table I where the data for $Y_2Cu_2O_5$ are taken from the report by Zhou and Navrotsky (*14*). In Fig. 7, the heats of solution of 225 phases are plotted against $1/r$. Generally, the entire data set seems to be described by a linear function of $1/r$ (solid line in the figure). However, there are significant deviations from the solid line in the data for $Dy_2Cu_2O_5$ and $Y_2Cu_2O_5$ and five data points excluding two points for $Dy_2Cu_2O_5$ and $Ho_2Cu_2O_5$ seem to show better linear relationship (dotted line). Similar tendency was observed in ΔH_s of Ln_2O_3 (see Fig. 1). These phenomena appear to be correlated to each other.

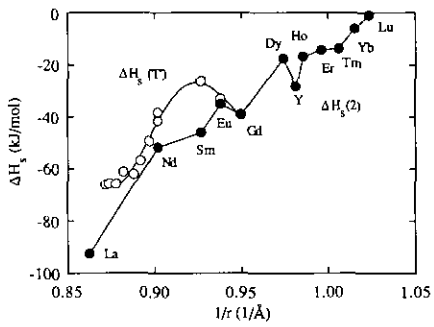

FIG. 6. Heats of solution of the T' phase, $\Delta H_s(T')$ and the mixture of Ln_2O_3 and CuO, $\Delta H_s(2) = \Delta H_s(Ln_2O_3) + \Delta H_s(\text{CuO})$ as functions of reciprocal of the ionic radius of Ln^{3+}.

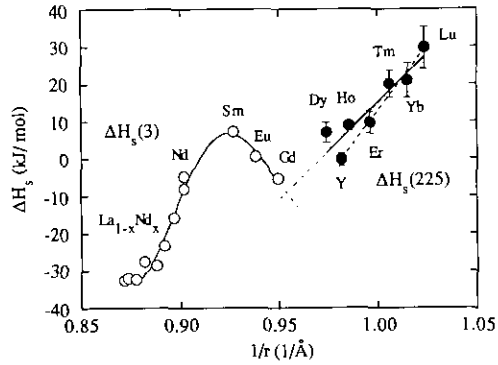

FIG. 7. Heats of solution of $Ln_2Cu_2O_5$, $\Delta H_s(225)$ and the mixture of T'-Ln_2CuO_4 and CuO, $\Delta H_s(3) = \Delta H_s(T') + \Delta H_s(\text{CuO})$ as functions of reciprocal of the ionic radius of Ln^{3+}. The data for $Y_2Cu_2O_5$ are taken from Ref. (*14*). The solid straight line was obtained by linear fitting of entire data set for the 225 phases while the dotted line is a fit excluding the two data points for $Dy_2Cu_2O_5$ and $Ho_2Cu_2O_5$.

To see the stability relation between a 225 phase and a mixture of T'-Ln_2CuO_4 and CuO, the term, $\Delta H_s(3) = \Delta H_s(T') + \Delta H_s(\text{CuO})$ is plotted in Fig. 7. The $\Delta H_s(225)$ and $\Delta H_s(3)$ curves cross near Ln = Gd at a fairly large angle. This is consistent with synthesis experiments at ambient pressure which show that the 225 structure is unstable for Ln ions larger than Tb^{3+} but would decompose according to the reaction,

$$Ln_2Cu_2O_5 \rightarrow T'\text{-}Ln_2CuO_4 + CuO.$$

Heats of formation from oxides of the 225 phases (Table I) are slightly positive or close to zero which indicates positive entropy changes for the formation reaction as pointed out by Zhou and Navrotsky (*14*).

Conclusion

Heats of solution in molten $2PbO \cdot B_2O_3$ at 977 K, ΔH_s of the series of compounds, Ln_2O_3 (Ln = Nd–Lu), T'-Ln_2CuO_4 (Ln = Nd–Gd) and $Ln_2Cu_2O_5$ (Ln = Dy–Lu) were measured. Heats of solution of these systems seem, to greater or lesser extent, influenced by the crystal field stabilization energies of Ln^{3+} ions (CFSE). A nonlinear relation was observed between $\Delta H_s(Ln_2O_3)$ and reciprocal of ionic radius of Ln^{3+}, $1/r$ which suggests CFSE of Ln^{3+} in the range of $0 \sim 10$ kJ/mole $\cdot$ Ln^{3+}.

Heats of solution of T' phases increase with increasing $1/r$ until Ln = Sm then decrease for larger $1/r$ (smaller Ln^{3+} ion). This downturn is explained by the CFSE of Ln^{3+} and/or nonlinear change of lattice energy of the T' phase as a function of $1/r$. Heats of solution of $Ln_2Cu_2O_5$ phases also suggest the influence of the CFSE in the cases Ln = Dy, Ho.

The thermochemical data are compatible with the experimental stability relations at ambient pressure among phases, T'-Ln_2CuO_4, $Ln_2Cu_2O_5$, Ln_2O_3, and CuO. The stability relations at high pressures were roughly estimated from the present results but calorimetric studies for high-pressure T' phases are indispensable for further discussion.

Acknowledgments

This work was partly supported by STA, Japan (The Bilateral International Joint Research by Special Coordination Funds Promoting Science and Technology). The calorimetry at Princeton was supported by the U.S. Department of Energy (DE FG0289ER45394) and the National Science Foundation (DMR 89-12549). Valuable discussions with Drs. J. DiCarlo, Z. Zhou, A. Mehta, and L. Topor of Princeton University are much appreciated. One of the authors (ETM) expresses his thanks to Drs. H. Yamada and M. Akaishi of NIRIM for helpful suggestions on high-pressure synthesis.

References

1. Hk. Muller-Buschbaum and W. Wollschlager, *Z. Anorg. Allg. Chem.* **414,** 76 (1975).
2. Y. Tokura, H. Takagi, and S. Uchida, *Nature* **337,** 345 (1989).
3. H. Freund and Hk. Muller-Buschbaum, *Z. Naturforsch. B* **32,** 609 (1977).
4. H. Okada, M. Takano, and Y. Takeda, *Physica C* **166,** 111 (1990).
5. P. Bordet, J. J. Capponi, C. Chaillout, D. Chateigner, J. Chenavas, Th. Fournier, J. L. Hodeau, M. Marezio, M. Perroux, G. Thomas, and A. Varela, *Physica C* **193,** 178 (1992).
6. K. Mocala, A. Navrotsky, J. F. Bringley, and B. A. Scott, submitted for publication.
7. A. Navrotsky, *Phys. Chem. Minerals* **2,** 89 (1977).
8. J. Bularzik, A. Navrotsky, J. DiCarlo, J. Bringley, B. Scott, and S. Traill, *J. Solid State Chem.* **93,** 418 (1991).
9. Ph. Galez and G. Collin, *J. Phys. France* **51,** 579 (1990).
10. Lattice parameters of the T' compounds were taken from the following literature. Pr_2CuO_4, JCPDS Card 22-0245; Nd_2CuO_4, JCPDS Card 24-0777; Sm_2CuO_4, JCPDS Card 24-0998; Eu_2CuO_4, JCPDS Card 24-0399; Gd_2CuO_4, JCPDS Card 24-0422; Ln_2CuO_4 (Ln= Y, Dy, Ho, Er, Tm), Ref. (*4*).
11. M. S. Islam, M. Leslie, S. M. Tomlinson, and C. R. A. Catlow, *J. Phys. C* **21,** L109 (1988).
12. L. Eyring, *in* "Handbook on the Physics and Chemistry of Rare Earths" (K. A. Gschneidner, Jr., and L. Eyring, Eds.) Vol. 3, Chap. 27, North-Holland, Amsterdam (1984).
13. I. Barin, "Thermochemical Data of Pure Substances," Part II, p. 1389, VCH Verlagsgesellshaft, Weinheim, Germany (1989).
14. Z. Zhou and A. Navrotsky, *J. Mater. Res.*, **7,** 2920 (1992).
15. R. D. Shannon, *Acta Crystallogr. Sect. A* **32,** 751 (1976).
16. R. W. G. Wyckoff, "Crystal structures," 2nd ed., Vol. 2, Chap. V, Interscience, New York (1967).
17. K. B. Yatsimirskii and N. A. Kostromina, *Russ. J. Inorg. Chem.* **9,** 971 (1964).
18. P. George and D. S. McClure, *Prog. Inorg. Chem.* **1,** 408 (1959).
19. T. E. Warner, P. P. Edwards, W. C. Timms, and D. J. Fray, *J. Solid State Chem.* **98,** 415 (1992).
20. I. Barin, "Thermochemical data of pure substances," Part I, p. 483, VCH Verlagsgesellshaft, Weinheim, Germany (1989).
21. Lattice parameters are taken from Ref. (*10*) and the following literature. CuO, JCPDS Card 5-0661; $Y_2Cu_2O_5$, JCPDS Card 33-0511; $Dy_2Cu_2O_5$, JCPDS Card 33-0455; $Ho_2Cu_2O_5$, JCPDS Card 33-0458; $Er_2Cu_2O_5$, JCPDS Card 33-0456; $Tm_2Cu_2O_5$, JCPDS Card 34-0386; $Yb_2Cu_2O_5$, JCPDS Card 33-0507; $Lu_2Cu_2O_5$, JCPDS Card 34-0387; Ln_2O_3 (Ln = Y, Pr–Lu), Ref. (*16*).